Open Access

Enhanced UV Emission from ZnO on Silver Nanoparticle Arrays by the Surface Plasmon Resonance Effect

Xiao Wang[1*†] , Qiong Ye[1†], Li-Hua Bai[2], Xi Su[3], Ting-Ting Wang[1], Tao-Wei Peng[1], Xiao-Qi Zhai[1], Yi Huo[1], Hao Wu[3], Chang Liu[3], Yu-Yu Bu[1], Xiao-Hua Ma[1], Yue Hao[1] and Jin-Ping Ao[1*]

Abstract

Periodical silver nanoparticle (NP) arrays were fabricated by magnetron sputtering method with anodic aluminum oxide templates to enhance the UV light emission from ZnO by the surface plasmon resonance effect. Theoretical simulations indicated that the surface plasmon resonance wavelength depended on the diameter and space of Ag NP arrays. By introducing Ag NP arrays with the diameter of 40 nm and space of 100 nm, the photoluminescence intensity of the near band-edge emission from ZnO was twofold enhanced. Time-resolved photoluminescence measurement and energy band analysis indicated that the UV light emission enhancement was attributed to the coupling between the surface plasmons in Ag NP arrays and the excitons in ZnO with the improved spontaneous emission rate and enhanced local electromagnetic fields.

Keywords: Surface plasmons, Zinc oxide, Silver nanoparticle arrays, Anodic aluminum oxide templates

Introduction

Recently, surface plasmons (SPs) have attracted much attention. In particular, as the collective oscillations of free electrons around metal nanoparticles (NPs) surface, localized surface plasmons (LSPs) were widely applied to enhance the light emission in optoelectronic devices, due to selective photon absorptions and enhanced local electromagnetic field around the metal NPs [1]. Many efforts of LSP-enhanced emissions have been made in ultraviolet (UV) optoelectronic devices such as light emitting diodes [2–4] and photodetectors [5–9].

ZnO is one of the most promising materials for UV optoelectronic devices due to a direct wide bandgap of 3.37 eV and an exciton binding energy of 60 meV [10]. However, the low UV light emission efficiency blocks its

commercial application. Hence, different metals (Ag [11–18], Au [12, 15, 19, 20], Al [21–24], Cu [25], Ti [26, 27], Ni [27], Pt [28]) with different shapes (gratings, sphere, cylinder, triangular prism, tetragonal prism, bowtie) have been applied to enhance the near band-edge UV emission of ZnO. Among them, Ag NPs with a sphere shape composited by hydrothermal method were most widely used due to relatively easy fabrication and effective light emission enhancement. However, hydrothermally composited Ag NPs are usually randomly distributed, and it is hard to control the local electromagnetic fields distribution and wafer homogeneity. Therefore, electron beam lithography (EBL) and nanoimprint lithography were applied to obtain controllable shapes and arrangements. Nevertheless, expensive facility and difficult in large-scale manufacturing block the applications of the EBL and nanoimprint lithography [24].

In this work, the LSP-enhanced UV light emissions from ZnO were obtained by introducing periodical Ag NPs arrays with AAO templates. The optimal size of Ag NP arrays was obtained as the diameter of 40 nm

*Correspondence: x.wang@xidian.edu.cn; jpao@xidian.edu.cn
†Xiao Wang and Qiong Ye have contributed equally to this work
¹ National Key Discipline Laboratory of Wide Band-Gap Semiconductor, School of Microelectronics, Xidian University, Xi'an 710071, People's Republic of China
Full list of author information is available at the end of the article

Wang *et al. Nanoscale Res Lett*   (2021) 16:8

Page 2 of 7

and space of 100 nm with a twofold photoluminescence enhancement in the UV light emission of ZnO. The simulation and experimental photoluminescence spectra were analyzed to reveal the mechanism of light emission enhancement.

Methods

The fabrication process is shown in Fig. 1. Firstly, commercial AAO templates were transferred on silicon substrate. The thickness of AAO templates is 200 nm with the diameter and space shown in Table 1. Sample 1 was fabricated without AAO templates and corresponding Ag NP arrays. Secondly, an Ag (35 nm) layer was deposited by magnetron sputtering with DC power of 100 W, pressure of 3 mTorr and Ar flow rate of 18 sccm. Thirdly, the AAO templates were removed by Kapton tape and Ag NP arrays were left on Si substrate. Finally, Al_2O_3 (10 nm) and ZnO (70 nm) films were in-turn grown on Ag NP arrays at 150 °C by atomic layer deposition (ALD), with trimethylaluminum (TMA), H_2O and diethyl zinc (DEZn) as the sources of aluminum, oxygen and zinc, respectively. The growth details and characteristics of ZnO films can be found in our previous publication [29].

The morphologies of AAO templates and Ag NP arrays were characterized by scanning electron microscope (SEM). The photoluminescence (PL) measurement was performed with a He-Cd laser ($\lambda = 325$ nm). The time-resolved PL spectra were measured with excitation

Table 1 The diameters and spaces of samples

Samples	Diameter (nm)	Space (nm)
1	–	–
2	30	65
3	40	65
4	40	100
5	60	100
6	70	125

wavelength at 310 nm at room temperature to evaluate the light emission mechanism.

Results and Discussion

Before conducting the experiments, numerical calculations by the finite-difference time-domain (FDTD) method were performed to analyze the effect of different diameters and spaces of Ag NP arrays on the electric field distribution and surface plasmon resonance wavelengths. The electric field distributions and the scattering cross-section (Q_{scat}) spectra of Ag NP arrays were simulated under a total-field scattered-field (TFSF) light source polarized along the z-axis. The analysis group was placed outside of the optical source to monitor the scattering cross section of light. The optical parameters of Ag were selected as the CRC model from the material database of the Lumerical FDTD solutions software. The simulated spatial electric field distribution in the sample
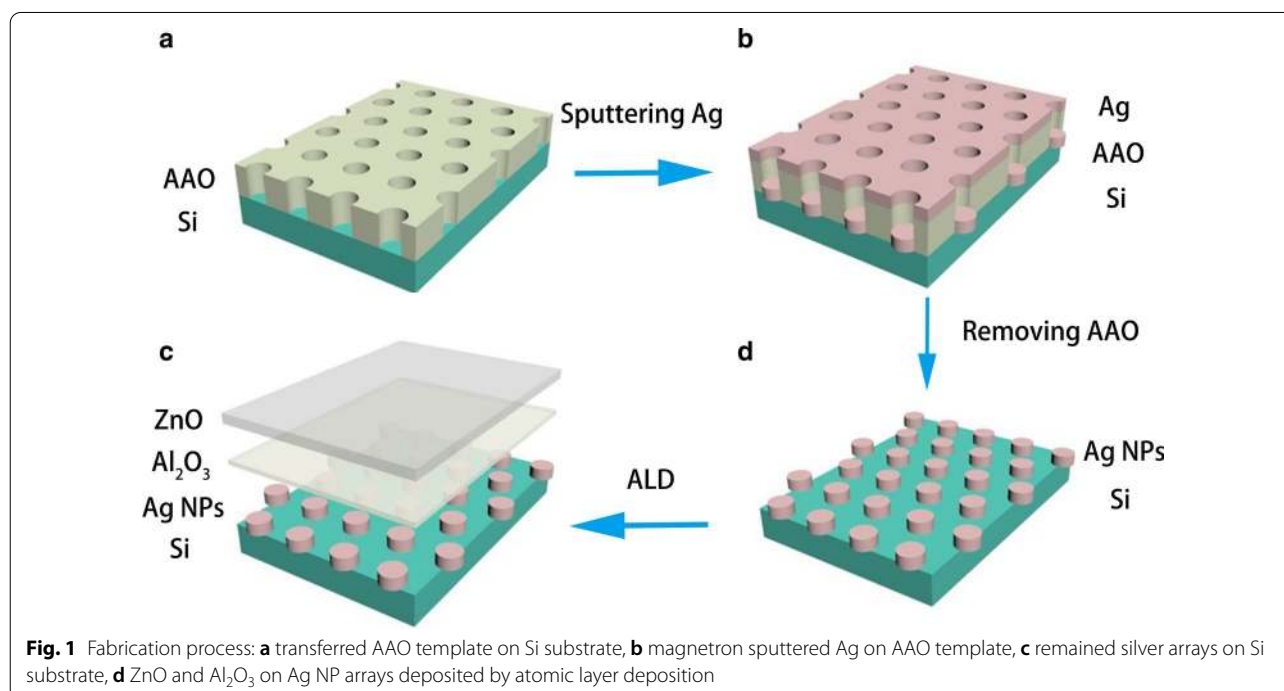

Fig. 1 Fabrication process: **a** transferred AAO template on Si substrate, **b** magnetron sputtered Ag on AAO template, **c** remained silver arrays on Si substrate, **d** ZnO and Al_2O_3 on Ag NP arrays deposited by atomic layer deposition

Wang *et al. Nanoscale Res Lett*   (2021) 16:8

Page 3 of 7

4 with the diameter of 40 nm and space of 100 nm is shown in Fig. 2a. The local electromagnetic field around the Ag NPs was enhanced about 3.5 times, leading to a strong coupling between the excitons in ZnO films and the SPs in Ag NP arrays, and resulting the light emission enhancement. Figure 2b shows the normalized Q_{scat} spectra of Ag NP arrays with different diameters and spaces. The surface plasmon resonance wavelengths of Ag NP arrays from sample 2 to sample 6 are 379, 399, 381, 402 and 408 nm, respectively. Considering the NBE emission of ZnO films around 383 nm, the optimized diameter and space of Ag NP arrays should be 40 and 100 nm in sample 4. By increasing the size of Ag NP arrays from sample 2 to 3, or from sample 4 to 5, the surface plasmon resonance wavelength makes a redshift under the same space condition. By increasing the space of Ag NP arrays from sample 3 to 4, the surface plasmon resonance wavelength makes a blueshift under the same diameter condition. Hence, the surface plasmon resonance wavelength of the Ag NP arrays depends on both the diameter and space of Ag NP arrays.

In Fig. 3, the transferred AAO templates and corresponding Ag NP arrays are demonstrated in the SEM images. As shown in Fig. 3a, c, e, g, i, the average diameters of AAO templates from sample 2 to sample 6 are measured to be 33, 38, 40, 61 and 71 nm, and the corresponding average spaces of AAO templates are 63, 61, 100, 101, 124 nm, which is in accord with the designed diameters and spaces in Table 1. As shown in Fig. 3b, d, f, h, j, the average diameters of Ag NP arrays from sample 2 to sample 6 are measured to be 8, 37, 46, 64 and 79 nm, and the corresponding average spaces of Ag NP arrays are 59, 62, 99, 102, 122 nm. When the diameter

of AAO template is as small as 33 nm, it is hard to form periodic Ag NP arrays. As for the diameters of AAO templates ranging from 40 to 60 nm in sample 3, 4 and 5, the diameters of Ag NP arrays are in accord with these of AAO templates. When the diameter of AAO template is as big as 71 nm, the diameter of sputtered Ag NP arrays is slightly bigger than that of AAO template, which may be on account of the Ag NP dispersion at the removing of the Kapton tape. Generally, the measured Ag NP array spaces are well matched with the AAO template spaces and in accord with the designed sizes. And the obtained periodic Ag NP arrays can be accurately controlled by applying the corresponding AAO templates.

Figure 4 presents the PL spectra of different samples at room temperature. As shown, a dominant peak at 383 nm and a weak peak at around 520 nm are obtained in the PL spectra, which are attributed to the near band-edge (NBE) emission and deep-level emission of ZnO, respectively. The deep-level emission was attributed to the oxygen vacancies [29]. The intensity ratio between the NBE peak and the deep-level peak was calculated to be 14 in the sample 1 without Ag NP arrays, indicating that ZnO films grown by ALD are in a good quality. The NBE peak intensities with Ag NP arrays are higher than that without Ag NP arrays, which is attributed to the coupling between the excitons in ZnO films and the SPs in Ag NP arrays, enhancing the local electromagnetic fields and increasing the spontaneous emission rate of ZnO. Among the PL curves of samples with different diameters and spaces, the NBE peak intensity in the sample 4 with the diameter of 40 nm and space of 100 nm is the strongest, which is twofold larger than that of sample 1 without Ag NP arrays, indicating that Ag NP arrays with the
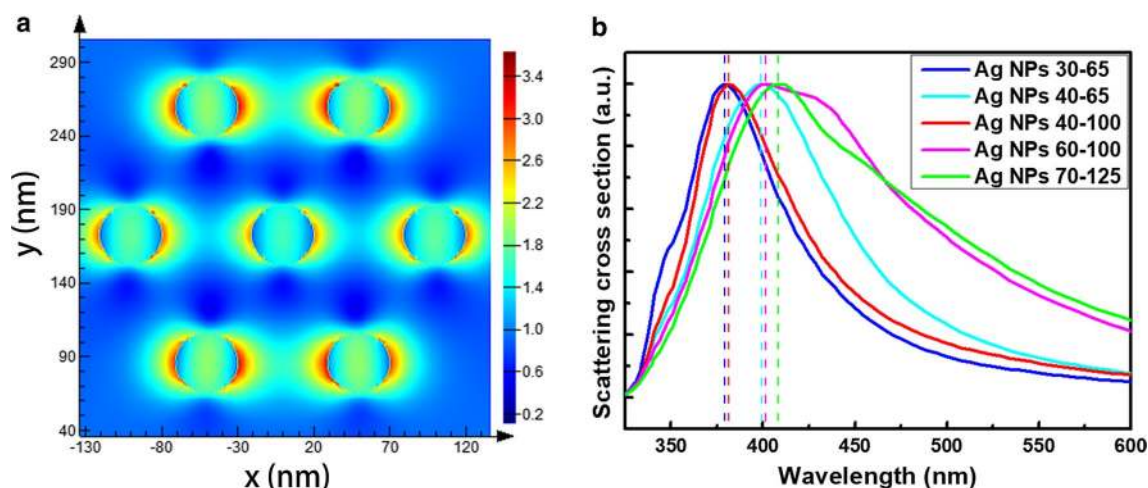

Fig. 2 **a** Simulated spatial electric field distribution in the sample 4 with the diameter of 40 nm and space of 100 nm. **b** Normalized scattering cross section spectra of Ag NP arrays with different diameters and spaces
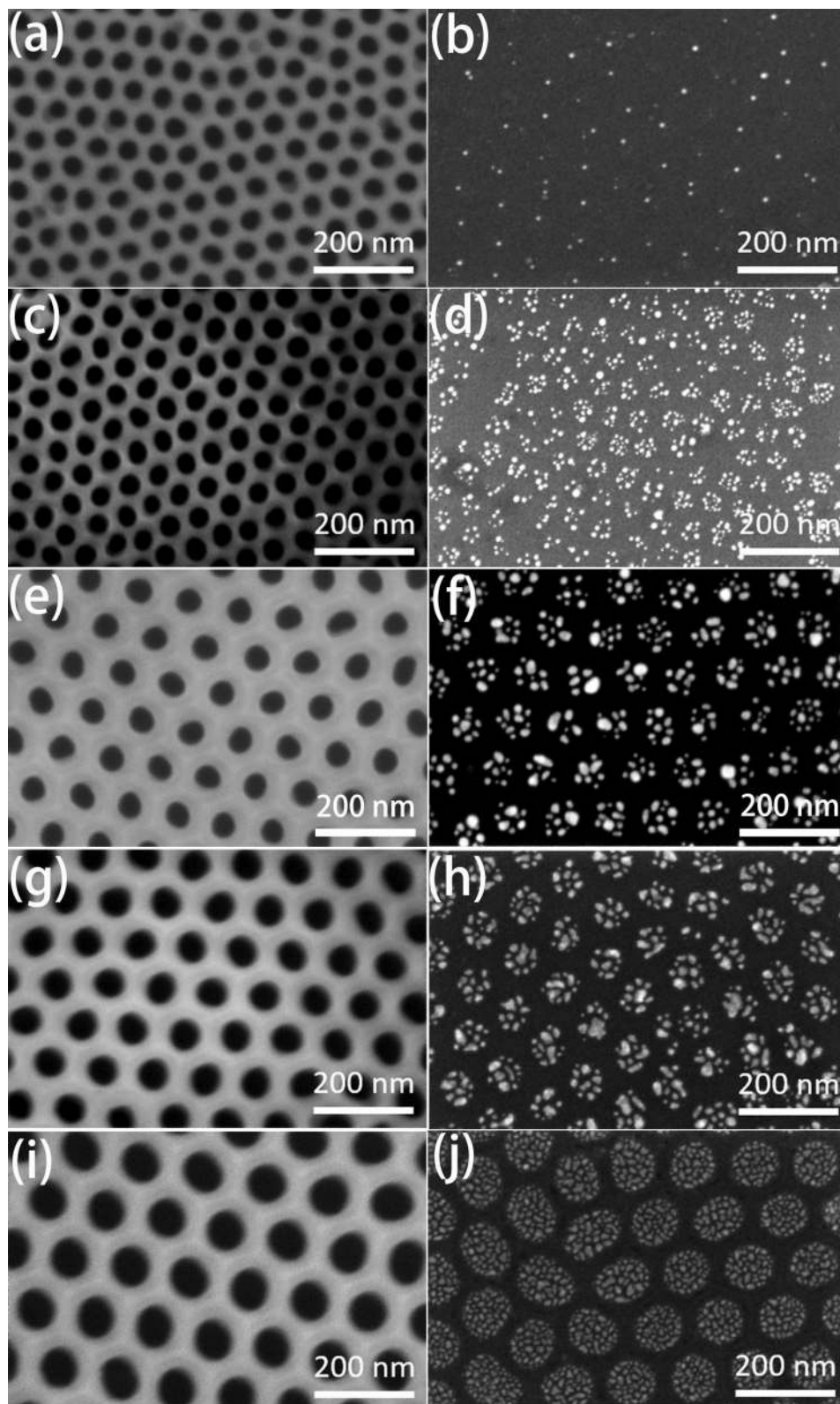
Wang *et al. Nanoscale Res Lett*   *(2021) 16:8*

Page 4 of 7

Fig. 3 SEM images of transferred AAO templates of **a** sample 2, **c** sample 3, **e** sample 4, **g** sample 5, **i** sample 6, and corresponding Ag NP arrays of **b** sample 2, **d** sample 3, **f** sample 4, **h** sample 5, **j** sample 6
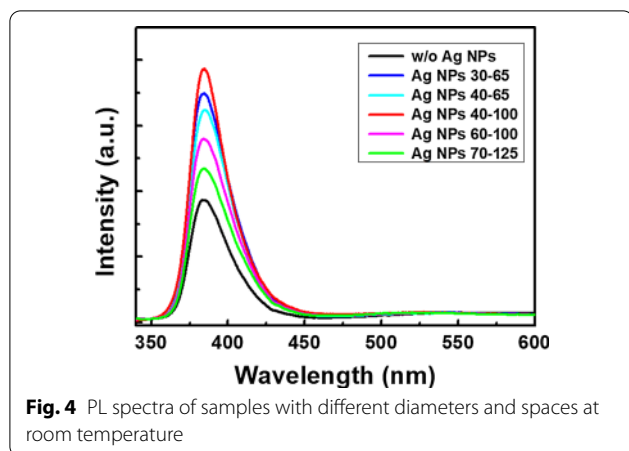
Wang *et al. Nanoscale Res Lett* (2021) 16:8

Page 5 of 7

Fig. 4 PL spectra of samples with different diameters and spaces at room temperature

diameter of 40 nm and space of 100 nm are the optimum to enhance the light emission of ZnO, which is in accord with the simulation results above. Besides, the deep-level peak at around 520 nm was almost the same for all samples, leading to a high intensity ratio of 28 between the NBE peak and the deep-level peak in the sample 4.

To further analyze the mechanism of the enhanced UV light emission by adding Ag NP arrays, the time-resolved PL decays of sample 1 without Ag NP arrays and sample 2 with Ag NP arrays were performed at room temperature in Fig. 5. The decay curves are fitted with an exponential decay model to obtain the decay lifetimes (τ) with the equation $I(t) = I_0 \exp(-t/\tau)$. The decay lifetimes of sample 1 without Ag NP arrays and sample 2 with Ag NP arrays are deduced to be 1.49 and 1.24 ns, respectively. The reduced decay lifetime from 1.49 to 1.24 ns indicates a faster decay process in the ZnO with Ag NP arrays, which may attribute to the improved spontaneous emission rate by adding Ag NP arrays, enhancing the coupling
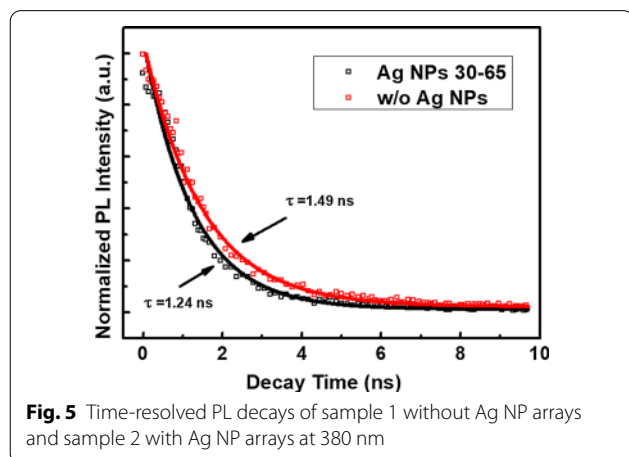
between the SPs in Ag NP arrays and the excitons in ZnO.

To further explain the improvement of the UV light emission, the energy band diagram of the Ag/Al_2O_3/ZnO structure is shown in Fig. 6. The work function of Ag is 4.26 eV and the electron affinity of ZnO is 4.35 eV, leading to a conduction band downward bending of ZnO near the Al_2O_3/ZnO interface. The 10-nm Al_2O_3 layer was applied to block Förster-type non-radiative energy transfer process from semiconductor to metal [28]. Due to the surface plasmons generated between the metal and dielectric medium at the Ag/Al_2O_3 interface, the local electric field near Ag NP arrays is enhanced, increasing the excitation energy density of incident light and the number of absorbed photons within the coupling distance. Simultaneously, the enhanced local electric field also promotes the surface plasmons of Ag NPs coupling with excitons of ZnO, which will improve the spontaneous emission rate and enhance the photoluminescence intensity of ZnO. Besides, there may be another process that electrons in the Ag NP arrays jump to the SPR level and then transfer to the conduction band of the ZnO [28]. And the increased electron density in the conduction band will also enhance the NBE emission of ZnO.

Conclusions

In summary, periodical Ag NP arrays were fabricated by magnetron sputtering method with AAO templates to enhance the UV light emission from ZnO by the surface plasmon resonance effect. Theoretical simulations indicated that the surface plasmon resonance wavelength depended on both the diameter and space of Ag NP arrays. By introducing Ag NP arrays with the diameter of 40 nm and space of 100 nm, the photoluminescence intensity of the near band-edge emission from ZnO was
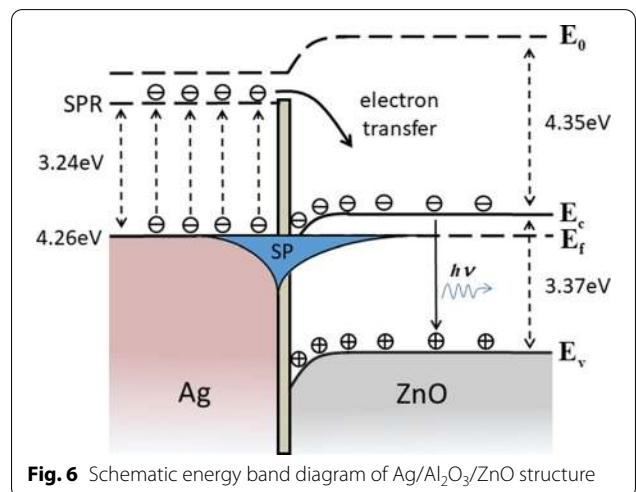

Fig. 5 Time-resolved PL decays of sample 1 without Ag NP arrays and sample 2 with Ag NP arrays at 380 nm

Fig. 6 Schematic energy band diagram of Ag/Al_2O_3/ZnO structure

Wang *et al. Nanoscale Res Lett*   (2021) 16:8

Page 6 of 7

twofold enhanced. Time-resolved photoluminescence measurement and energy band analysis revealed that the improvement of UV light emission was attributed to the coupling between the SPs in Ag NP arrays and the excitons in ZnO with the improved spontaneous emission rate and enhanced local electromagnetic fields.

Abbreviations
NP: Nanoparticle; AAO: Anodic aluminum oxide; SPs: Surface plasmons; LSPs: Localized surface plasmons; UV: Ultraviolet; ALD: Atomic layer deposition; SEM: Scanning electron microscope; PL: Photoluminescence; FDTD: Finite-difference time domain.

Authors' contributions
XW conceived the project and drafted the manuscript. QY, LHB and XS performed the simulation and experiments. TTW, TWP, XQZ and YH participated in the data analysis. HW, CL, YYB, XHM and YH participated in the project design. JPA supervised the overall study. All authors read and approved the final manuscript.

Availability of Data and Materials
The experiment data supporting the conclusion of this manuscript have been given in this manuscript. All data are fully available without restriction.

Competing interests
The authors declare that they have no competing interests.

Author details
[1] National Key Discipline Laboratory of Wide Band-Gap Semiconductor, School of Microelectronics, Xidian University, Xi'an 710071, People's Republic of China. [2] School of Science, Xi'an Shiyou University, Xi'an 710065, People's Republic of China. [3] Key Laboratory of Artificial Micro- and Nanostructures of Ministry of Education, School of Physics and Technology, Wuhan University, Wuhan 430072, People's Republic of China.

References
1. Barnes WL, Dereux A, Ebbesen TW (2003) Surface plasmon subwavelength optics. Nature 424:824–830
2. Bie YQ, Liao ZM, Wang PW, Zhou YB, Han XB, Ye Y, Zhao Q, Wu XS, Dai L, Xu J, Sang LW, Deng JJ, Laurent K, Leprince-Wang Y, Yu DP (2010) Single ZnO nanowire/p-type GaN heterojunctions for photovoltaic devices and UV light-emitting diodes. Adv Mater 22:4284–4287
3. Lupan O, Pauporte T, Viana B (2010) Low-voltage UV-electroluminescence from ZnO-nanowire array/p-GaN light-emitting diodes. Adv Mater 22:3298–3302
4. Yang Q, Wang W, Xu S, Wang ZL (2011) Enhancing light emission of ZnO microwire-based diodes by piezo-phototronic effect. Nano Lett 11:4012–4017
5. Liu Y, Zhang X, Su J, Li H, Zhang Q, Gao Y (2014) Ag nanoparticles@ ZnO nanowire composite arrays: an absorption enhanced UV photodetector. Opt Express 22:30148–30155
6. Biswas P, Cho SR, Kim JW, Baek SD, Myoung JM (2017) Improved UV response of ZnO nanotubes by resonant coupling of anchored plasmonic silver nanoparticles. Nanotechnology 28:225502
7. Khan R, Uthirakumar P, Kim TH, Lee IH (2019) Enhanced photocurrent performance of partially decorated Au nanoparticles on ZnO nanorods based UV photodetector. Mater Res Bull 115:176–181
8. Cai Y, Wang Z, Yan S, Ye L, Zhu J (2018) Ultraviolet absorption band engineering of graphene by integrated plasmonic structures. Opt Mater Express 8:3295–3306
9. Guo Y, Wang S, Zhou Y, Chen C, Cai Y (2019) Broadband absorption enhancement of graphene in the ultraviolet range based on metal-dielectric-metal configuration. J Appl Phys 126:213103
10. Wang X, Bai L, Zhang H, Su X, Wu H, Liu C (2018) Ag nanoparticle surface-plasmon-resonance-enhanced electroluminescence from semipolar n-ZnO/p-GaN heterojunction light-emitting diodes. Appl Phys Express 11:102101
11. Gwon M, Lee E, Kim DW, Yee KJ, Lee MJ, Kim YS (2011) Surface-plasmon-enhanced visible-light emission of ZnO/Ag grating structures. Opt Express 19:5895
12. Guidelli EJ, Baffa O, Clarke DR (2015) Enhanced UV emission from silver/ZnO and Gold/ZnO core–shell nanoparticles: photoluminescence, radio-luminescence, and optically stimulated luminescence. Sci Rep 5:14004
13. Abbass AE, Swart HC, Kroon RE (2017) Non-plasmonic enhancement of the near band edge luminescence from ZnO using Ag nanoparticles. J Lumin 182:263–267
14. Khomchenko V, Sopinskyy M, Mazin M, Danko VA, Lytvyn OS, Piryatinskii Y (2019) The violet luminescence band in ZnO and ZnO-Ag thin films. J Lumin 213:519–524
15. Thinh VD, Lam VD, Bach TN, Van ND, Manh DH, Tung DH, Lien NTH, Thuy UTD, Anh TX, Tung NT, Le NTH (2020) Enhanced optical and photocatalytic properties of Au/Ag nanoparticle-decorated ZnO films. J Electron Mater 49:2625–2632
16. Chen C, Chen J, Zhang J, Wang S, Zhang W, Liang R, Dai J, Chen C (2016) Ag-decorated localized surface plasmon-enhanced ultraviolet electroluminescence from ZnO quantum dot-based/GaN heterojunction diodes by optimizing MgO interlayer thickness. Nanoscale Res Lett 11:1–6
17. Yao YC, Yang ZP, Hwang JM, Chuang YL, Lin CC, Haung JY, Chou CY, Sheu JK, Tsai MT, Lee YJ (2016) Enhancing UV-emissions through optical and electronic dual-function tuning of Ag nanoparticles hybridized with n-ZnO nanorods/p-GaN heterojunction light-emitting diodes. Nanoscale 8:4463–4474
18. Kuiri PK, Pramanik S (2018) Large enhancement of UV luminescence emission of ZnO nanoparticles by coupling excitons with Ag surface plasmons. J Appl Phys 123:154302
19. Li L, Wang CY, Han F, Yang SM, Jing WX, Jiang ZD (2018) Largely enhanced near band edge emission of ultrathin zinc oxide nanowire/gold nanoparticles composites by surface plasmon resonance. Appl Surf Sci 433:1154–1157
20. Qin FF, Xu CX, Zhu QX, Lu JF, You DT, Xu W, Zhu Z, Manohari AG, Chen F (2018) Extra green light induced ZnO ultraviolet lasing enhancement assisted by Au surface plasmons. Nanoscale 10:623–627
21. Norek M, Łuka G, Włodarski M (2016) Plasmonic enhancement of UV emission from ZnO thin films induced by Al nano-concave arrays. Appl Surf Sci 384:18–26
22. Dellis S, Kalfagiannis N, Kassavetis S, Bazioti C, Dimitrakopulos GP, Koutsogeorgis DC, Patsalas P (2017) Photoluminescence enhancement of ZnO via coupling with surface plasmons on Al thin films. J Appl Phys 121:103104
23. Fiedler S, Lem LOLC, Ton-That C, Schleuning M, Hoffmann A, Phillips MR (2020) Correlative study of enhanced excitonic emission in ZnO coated with Al nanoparticles using electron and laser excitation. Sci Rep 10:1–9
24. Zhang H, Su X, Wu H, Liu C (2019) Surface plasmon-enhanced UV-emission from ZnO by aluminum bowtie nanoantenna arrays. J Alloys Compd 772:460–464
25. Ren QH, Zhang Y, Wang T, Yu WJ, Ou X, Lu HL (2019) Facile synthesis and photoluminescence mechanism of ZnO nanowires decorated with Cu nanoparticles grown by atomic layer deposition. ACS Appl Electron Mater 1:1616–1625
26. Li L, Yao C, Gan J, Jiang K, Hu Z, Lin J, Xu N, Sun J, Wu J (2020) Large enhancement and its mechanism of ultraviolet emission from ZnO

Wang *et al. Nanoscale Res Lett*   (2021) 16:8

Page 7 of 7

nanorod arrays at room and low temperatures by covering with Ti coatings. J Phys Chem C 124:4827–4834

27. Patra N, Karuturi SK, Vasa NJ, Nakamur D, Higashihata M, Singh V, Palani IA (2019) Influence of Ni, Ti and NiTi alloy nanoparticles on hydrothermally grown ZnO nanowires for photoluminescence enhancement. J Alloys Compd 770:1119–1129

28. Ren QH, Zhang Y, Lu HL, Chen HY, Zhang Y, Li DH, Liu WJ, Ding SJ, Jiang AQ, Zhang DW (2016) Surface-plasmon mediated photoluminescence enhancement of Pt-coated ZnO nanowires by inserting an atomic-layer-deposited Al_2O_3 spacer layer. Nanotechnology 27:165705

29. Wang T, Wu H, Chen C, Liu C (2012) Growth, optical, and electrical properties of nonpolar m-plane ZnO on p-Si substrates with Al_2O_3 buffer layers. Appl Phys Lett 100:011901

Publisher's Note